Available online at www.sciencedirect.com
SCIENCE DIRECT
Catalysis Today 114 (2006) 248–256
CATALYSIS TODAY
www.elsevier.com/locate/cattod

The effect of immobilization/mobilization processes on the temperature onset of a catalyst bed production studied with ethylene oligomerization on HZSM-5 zeolites

A. Zikánová [a], M. Derewiński [b], P. Sarv [c], P. Hudec [d], P. Hrabánek [a], M. Kočiřík [a,*]

[a] *J. Heyrovský Institute of Physical Chemistry, Academy of Sciences of the Czech Republic, Dolejškova 3, 182 23 Prague, Czech Republic*
[b] *Institute of Catalysis and Surface Chemistry, Polish Academy of Sciences, Niezapominajek 8, 30-239 Cracow, Poland*
[c] *Institute of Chemical Physics and Biophysics, Estonian Academy of Sciences, Akadeemia 23, EE0023 Tallin, Estonia*
[d] *Department of Petroleum Technology and Petrochemistry, Slovak University of Technology, Radlinského 9, 812 37 Bratislava, Slovak Republic*

Available online 23 March 2006

Abstract

Immobilization of ethylene in the channel system of HZSM-5 was evaluated from the breakthrough curves of ethylene and desorption curves of ethylene transformation products measured on a zeolite bed between 308 K and 523 K. The kinetics of the overall immobilization/mobilization reaction was measured on a series of HZSM-5 samples in an integral flow reactor with a fixed bed of zeolite at 623 K. The aluminum content of the samples ranged from 3.2 to 6.4 Al atoms per unit cell. The zeolites were characterized by XRD, SEM, chemical analysis, ^{27}Al MAS NMR, water sorption, TPD of NH_3 and FTIR spectroscopy. The results of kinetic measurements are represented by a family of S-shaped curves plotted as ethylene conversion versus contact time. The form of the curves suggests a contribution of an autocatalytic rate step to the kinetics. The length of the induction period increases with increasing crystal size and decreasing aluminum content in the catalyst. The kinetic curves obtained for crystals of the same aluminum content are strongly influenced by the crystal size. The ethylene breakthrough curves exhibit at the beginning a sharp breakthrough peak which decreases with accelerating oligomerization. The temperature threshold of zeolite bed production was estimated to lie at 418 K. At this temperature C_2–C_5 hydrocarbons were found in the gas phase in the gas leaving the reactor. The curve plotted as the amount of immobilized species against the temperature of the zeolite bed exhibits a steep increase to a flat maximum occurring between 353 K and 433 K, followed by a steep decrease. Adsorption of water on samples loaded with the immobilized species provides information about the space accessible from the gas phase and indicates differences in the nature of immobilized species formed at different temperatures.

Keywords: HZSM-5; Ethylene; Oligomerization; Immobilization/mobilization; Sorption and reaction dynamics

1. Introduction

To our knowledge no systematic studies of immobilization/mobilization rate processes have been performed with microporous materials where specific immobilization mechanisms may manifest themselves. Immobilization phenomena in zeolitic catalysts, sorbents and membranes are of particular interests. Results of several recent investigations in this area are summarized below.

Anomalous patterns of sorption (desorption) kinetic curves found for zeolites of MFI-type structure in studies [1–5] may be considered an indication of immobilization of molecules in the zeolite channel system. Authors of the above studies were unable to describe these patterns by the model of pure Fickian diffusion because in long-term experiments the experimental curves measured at constant boundary conditions strongly deviated from those calculated from the solution of the second Fick law. Some possible cases of immobilization of molecules in MFI-type zeolites were specified in Refs. [2,3,6,7].

Immobilization via chemical transformation of mobile molecules into immobile species of large critical dimensions and low mobility appears to be of special importance. Immobilization has been indicated in the system *p*-ethyltoluene-HZSM-5, where it was apparently caused by the formation of the corresponding meta-form [2]. Mobilization of a layer adsorbed on H-ZSM-5 zeolite and represented by a

* Corresponding author.
E-mail address: kocirik@jh-inst.cas.cz (M. Kočiřík).

0920-5861/$ – see front matter
doi:10.1016/j.cattod.2006.01.002

mixture of para- and meta-ethyltoluene has been described in [8]. It followed from that study that the temperature at which the transformed species appeared in the reaction product was that corresponding to mobilization of the adsorption layer in zeolite channels due to the proceeding chemical transformation. Thus, the rate of immobilization and mobilization of ethyltoluenes appears to be limited by the respective isomerization rates.

Another immobilization/mobilization mechanism may be associated with addition or decomposition reactions. Typical examples of mobilization reactions belonging to this class are those involved in removal of organic templates such as tetraalkylammonium (TAA^+) cations or bulky amines from zeolite channels by pyrolysis. For crystals containing TAA^+ the mobilization reactions involve a Hoffmann-type reaction and β-elimination reactions. Template removal by thermal treatment of as-synthesized zeolites was systematically investigated, e.g. by Parker et al. [9] and also by Kessler and coworkers [10–14].

By generalizing the above phenomena we have been led to a hypothesis that for some selected classes of chemical transformations proceeding on microporous catalysts the temperature onset of catalyst bed production is determined by mobilization of an adsorbed layer of product precursors formed within the microporous system. As a result of such a behavior the values of Stefan-Maxwell single-component diffusivities $Đ_i$ [15], which enter into the models of reaction kinetics controlled by intracrystalline diffusion, could not be estimated by extrapolation of diffusivities obtained from low-temperature single-component sorption experiments to a temperature region above the onset of catalyst bed production. Thus, alternative approaches based on physical methods used to observe mobilities of sorbed species in multicomponent mixtures combined with molecular simulation are of increasing importance.

Based on an extensive literature dealing with the properties of ethylene complexes and the behavior of ethylene oligomers in the channel system of MFI-type zeolites [16–25] we decided to test the above hypothesis and analyze the corresponding immobilization and mobilization mechanism on ethylene oligomerization on HZSM-5 zeolites.

2. Experimental

2.1. Materials

Two series of catalysts were used: (i) Commercially available MFI-type materials PQ Corp. (CONTEKA) denoted CBV-3020 (samples 18z, 20z) and 5020 (sample 21z) and (ii) those produced by the Research Institute for Petroleum and Hydrocarbon Gases, Bratislava (VURUP) (samples 52, 53, 55 and 56). The PQ Corp. (CONTEKA) materials were supplied in hydrogen form whereas those obtained from VURUP in ammonium one.

The zeolite samples were pressed to wafers, ground and sieved to get a fraction of 0.18–0.30 mm. Prior to the catalytic and sorption experiments the zeolite samples were calcined at 823 K for 5 h in a stream of dry oxygen (oxygen flow rate 150 ml/min). The apparent density ρ_{app} of the catalyst granules and the bulk density ρ_b of the bed packing were estimated for the dry samples.

Ethylene used in the experiments was supplied by Linde Technoplyn a.s. It was of 99.8% purity and was dried over molecular sieves before use.

2.2. Experimental techniques

2.2.1. Characterization of zeolites

TPD of ammonia pre-adsorbed at 423 K was used to estimate the total amount of the strong acid sites (Brønsted and Lewis). Water sorption was measured gravimetrically (at $p/p_s = 0.26$ and $T = 298$ K) on samples activated prior to the catalytic measurements, and the number $N^0_{H_2O}$ of water molecules adsorbed per unit cell was estimated (the superscript "0" refers to measurement on activated samples). Another measurement of water adsorption was performed after the catalytic test, i.e., on samples loaded with the immobilized organic species. As a primary result of these experiments the observed change in the catalyst mass can be taken as a measure of adsorbed water, provided no displacement of organic species by water occurred. We denoted this apparent sorbed amount of water as N_{H_2O}. Thus, N_{H_2O} represents a lower estimate of the free space (and also of the number of accessible hydrophilic centers) in catalysts loaded with immobilized ethylene oligomers.

^{27}Al MAS NMR was used to establish the fraction of different aluminum species present in the zeolite samples. ^{27}Al MAS NMR spectra were recorded on Brucker AMX500 spectrometer in 11.7 T magnet at 130.28 MHz frequency. The length of the exciting pulse was 10° and the relaxation delay was 0.2 s. The nutation frequency of the exciting pulse was 70 kHz. The sample spinning speed ranged from 11 to 12 kHz. All ^{27}Al chemical shifts were referenced to 1 M aqueous solution of $Al(NO_3)_3$.

Crystallinity of the samples was estimated from XRD data obtained with the Siemens 5005 instrument; scanning electron microscopy (Philips XL 30) was used to determine the crystal size and morphology.

FTIR experiments were performed on self-supported discs of zeolites (about 15 mg cm^{-2}) with the Nicolet 800 spectrometer. Zeolites were activated at 823 K for 2 h in vacuo (10^{-4} Pa).

2.2.2. The catalytic tests

The catalytic tests were carried out in a flow reactor with an integral bed of the catalyst. Ethylene conversion was studied at temperatures between 308 K and 623 K. Most catalytic measurements were performed at 623 K with ethylene feed of $c_{et0}\upsilon_\Sigma = 1.15 \times 10^{-4}$ mol min^{-1}. The effect of ethylene concentration in the feed was also tested using ethylene feed $c_{et0}\upsilon_\Sigma = 2.1 \times 10^{-4}$ mol min^{-1} and $c_{et0}\upsilon_\Sigma = 0.6\,1 \times 10^{-4}$ mol min^{-1}. The contact time $\tau_{c\alpha}$ was varied between 0.03 s and 0.13 s (by changing the mass of the catalyst in the bed between about 80 and 1000 mg). Fresh catalyst was used for

each catalytic run. Ethylene conversion was measured at a steady state reached within 2–3 h on stream. The gaseous products were analyzed by GC using a FID detector. The hydrocarbon products were separated on a column packed with PORAPAK type Q supplied by Waters Assoc. Inc.

The conversion of ethylene was calculated from the formula:

$$x_{\mathrm{et}} = \frac{c_{\mathrm{et0}} - c_{\mathrm{et}}}{c_{\mathrm{et0}}} \quad (1)$$

where c_{et0} and c_{et} are molar concentrations of ethylene in the feed and the product, respectively.

The contact time $\tau_{c\alpha}$ was defined for the purposes of this study as:

$$\tau_{c\alpha} = \frac{\alpha V_{\mathrm{L}}}{\nu_{\Sigma}} = \left(\frac{m_{\mathrm{z}}}{\nu_{\Sigma}}\right)\left[\frac{1}{\rho_{\mathrm{b}}} - \frac{1}{\rho_{\mathrm{app}}}\right] \quad (2)$$

where α is the fraction of the intergranular volume of the bed, V_{L} the total volume of the bed, m_{z} the mass of the catalyst in the bed, and υ_{Σ} the volumetric flowrate of the gas mixture (ml/s).

2.2.3. Sorption and reaction dynamics of ethylene

The commercially available zeolite that exhibited the most reproducible catalytic properties (sample 20z) was chosen for further study of sorption and reaction dynamics of ethylene.

A fresh sample was used in each experiment. The experimental temperatures were between 308 K and 523 K and the contact time $\tau_{c\alpha}$ was approximately 0.13 s (zeolite amount ~1 g). The amount of the immobilized substance was determined from the breakthrough curves of C_2–C_5 hydrocarbons on the basis of mass balance in the bed. The breakthrough curves are defined as $W_{\mathrm{et}} = m_{\mathrm{et}}/m_{\mathrm{et0}}$ and $W_i = m_i/m_{\mathrm{et0}}$, where m_{et}, m_i represent the mass of the respective species in the sampling loop and the subscripts et and i (i = 3–5) refer to ethylene and C_i hydrocarbons. The quantity m_{et0} refers to the content of ethylene in the feed. The amount of ethylene units equivalent to the amount of species i in the product which left the bed during the time interval 0, t can be expressed as:

$$N_i = c_{\mathrm{et0}}\nu_{\Sigma}\int_0^t W_i\,\mathrm{d}t \quad (3)$$

The total amount of ethylene units N_{ethylene} (mol) immobilized in any form on the catalyst during the time interval $\langle 0,t\rangle$ can be calculated from the following formula:

$$N_{\mathrm{ethylene}} = c_{\mathrm{et0}}\nu_{\Sigma}\int_0^t \left[1 - \left(W_{\mathrm{et}} + \sum_i W_i\right)\right]\mathrm{d}t \quad (4)$$

3. Results and discussion

3.1. Catalysts characterization

XRD analysis showed that all MFI samples were highly crystalline with no other crystalline phase present, except for sample 20z (PQ Corp. CBV-3020), where a small amount of the side phase – Y type zeolite – was detected.

The SEM analysis confirmed the absence of non-reacted amorphous phases and revealed the difference in size and morphology of the crystals. Fig. 1 shows examples of scanning electron micrographs of the studied samples. The samples were investigated in the form of agglomerates (samples 18z, 20z, 21z, 53 and 56) or as individual crystals (samples 52 and 55). The size of the crystal particles estimated from SEM micrographs is summarized in Table 1.

Typical IR spectra of the activated samples (18z and 20z) in the OH stretching vibration region are shown in Fig. 2. In addition to the bands at 3745 cm^{-1} and 3609 cm^{-1}, attributed to the terminal silanols and bridging SiOHAl groups, a band at 3665 cm^{-1} is present in the spectra. This band reflects the presence of extraframework, octahedrally coordinated aluminum.

This is confirmed by the ^{27}Al MAS NMR data. Fig. 3 shows ^{27}Al MAS NMR spectra registered for the studied samples. Different types of aluminum can be distinguished: tetrahedrally coordinated framework Al (52.2–55.2 ppm) and extraframework octahedral Al (−0.7 to −0.5 ppm). The signal of the distorted tetrahedral Al sites with asymmetric surroundings (extraframework) can also be seen in the spectra as a shoulder on the peak of the framework Al (~36 ppm). The distribution of Al between the different species is shown in Table 1.

The number of adsorbed water molecules per U.C. on activated samples is correlated with the total number of aluminum atoms per U.C. estimated from elemental analysis. It is apparent from Fig. 4 that up to about four Al atoms/U.C. the dependence is approximately linear with about 5–6 H_2O molecules/Al. The form of the correlation is in accordance with the literature data [26]. The adsorbed amount of water was found to be essentially independent of the number of the framework, tetrahedral aluminum atoms, indicating that most types of the aluminum species present in the zeolite are associated with hydrophilic centers.

3.2. Ethylene conversion on the catalyst bed with a mobilized layer of sorbed species

Below 418 K no products of ethylene transformation were found at the outlet of the reactor. Starting from 418 K a conversion was observed and the main products detected were C_2, C_3, C_4 and C_5 hydrocarbons. Only a minor amount of higher hydrocarbons that was neglected in the mass balance has been found in the reaction mixture.

Fig. 5a shows the dependence of ethylene conversion at 623 K on the contact time for the zeolites produced by VURUP (samples 52, 53, 55 and 56). The plots are sigmoid with an induction period. The length of the induction period (or the position of the inflection point) depends strongly on the Al content and on the crystal size. As expected, zeolite samples with comparable total aluminum content but with smaller crystal size are more effective in ethylene conversion (cf. catalyst pairs 56/55 and 53/52). The observed dependence on crystal size may be due to a diffusion limitation and/or to a

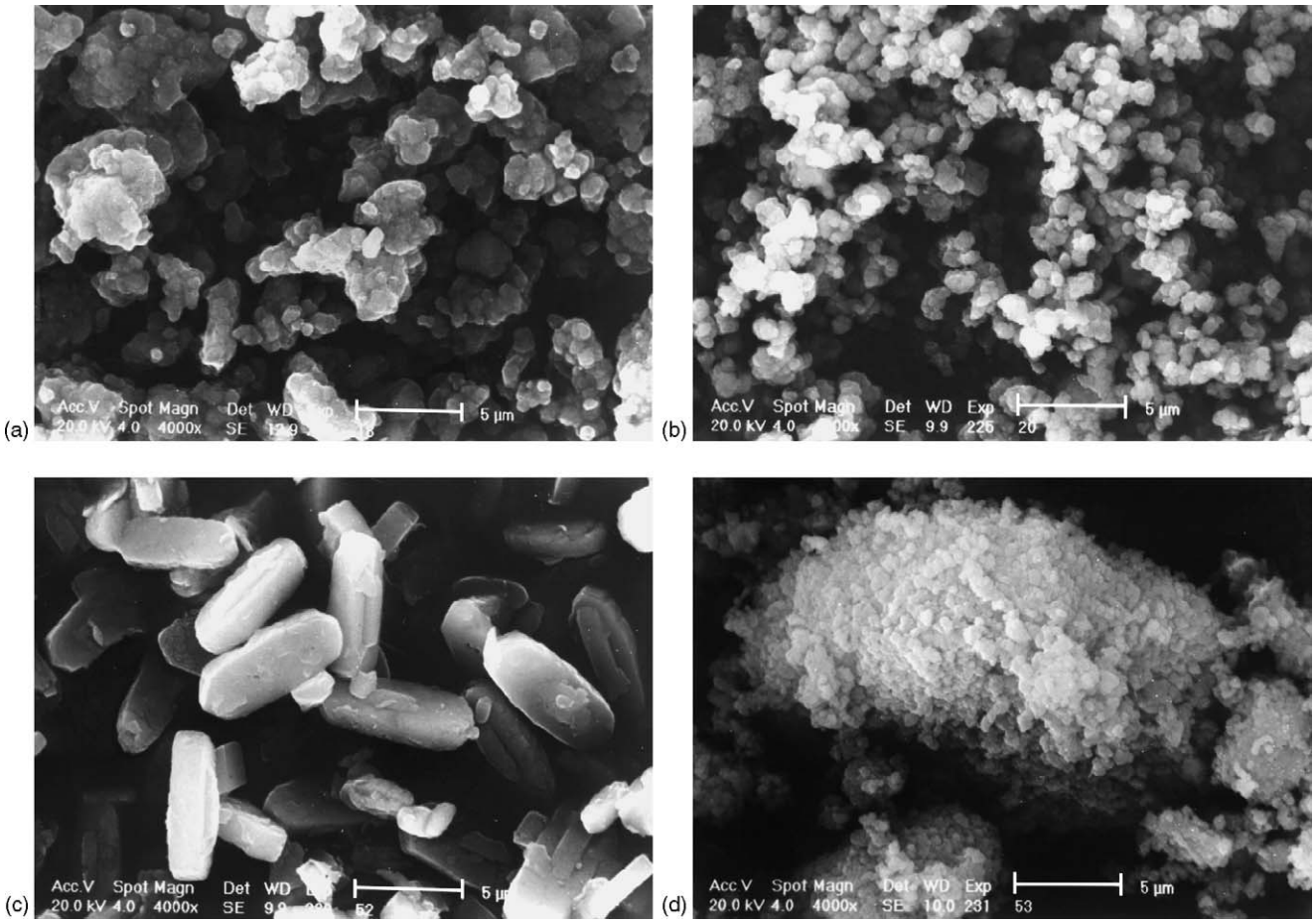

Fig. 1. Scanning electron micrographs of samples: a—18Z, b—20Z, c—52 and d—53.

significant contribution of the reaction at the external surface of the crystals, which is especially important for small crystals.

Fig. 5b shows the dependence of ethylene conversion on the contact time obtained at 623 K for the industrial catalysts (PQ, Conteka), samples 18z, 20z and 21z. The curves plotted as conversion versus contact time differ significantly between the samples with almost identical total aluminum contents (18z and 20z). The conversion achieved with 18z is considerably higher than that with 20z and there is an insignificant induction period on the conversion versus contact time curve for sample 18z.

The crystal size was approximately the same for all three preparations, i.e. substantially below 1 μm. The crystals are

Table 1
Characteristics of the catalysts

Sample specification, provenience	Crystal size, particle size (μm/μm)	$N_{\Sigma Al}$[b]/U.C.	x_{Al}[c]			N_{NH_3}[g]/U.C.	N_{H_2O}[h]/U.C.
			$^{IV}Al_{fram}$[d]	$^{IV}Al_{nonfram}$[e]	^{VI}Al[f]		
18z CONTEKA CBV-3020	0.1, 1–3	4.5	0.50	0.33	0.17	Not determined	24.0
20z PQ Corp. CBV-3020	0.1, 1–3	5.1	0.47	0.35	0.18	4.2	28.1
21z PQ Corp. CBV-5020	0.1, 1–3	3.2	0.61	0.27	0.12	3.1	20.4
52 VURUP[a]	6, –	4.1	0.91	0.03	0.06	4.0	23.5
53 VURUP[a]	<0.1, 1.9	4.2	0.78	0.10	0.08	3.6	23.5
55 VURUP[a]	3, –	6.4	0.68	0.18	0.14	5.2	31.2
56 VURUP[a]	<0.1	6.4	0.56	0.26	0.18	5.1	30.7

[a] VURUP—Research Institute for Petroleum and Hydrocarbon Gases, Bratislava.
[b] $N_{\Sigma Al}$—total number of aluminum atoms per U.C. based on elemental analysis.
[c] x_{Al}—fraction of respective Al species based on total number of aluminum atoms estimated from ^{27}Al MAS NMR analysis.
[d] $^{IV}Al_{fram}$—tetrahedrally coordinated, framework aluminium.
[e] $^{IV}Al_{nonfram}$—tetrahedrally coordinated, extralattice aluminium.
[f] ^{VI}Al—octahedrally coordinated, extraframework aluminum.
[g] N_{NH_3}—total number of NH_3 molecules per U.C. estimated from TPD of ammonia preadsorbed at 423 K.
[h] N_{H_2O}—total number of H_2O molecules per U.C. estimated from water sorption at 298 K and $p/p_s = 0.26$.

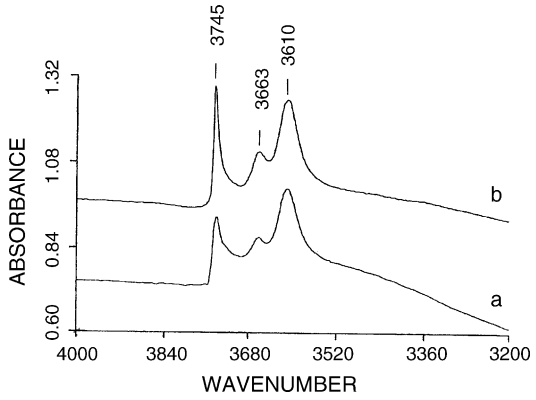

Fig. 2. IR spectra of the samples in OH stretching vibration region: (a) 18z, (b) 20z.

present in the samples in the form of agglomerates. The results do not allow us to make any conclusions concerning the exact reason underlying the different behavior of the industrial samples. In spite of the smaller amount of tetrahedrally coordinated framework Al–2.2 and 2.4 Al atoms per U.C. in samples 18z and 20z, respectively—the observed differences in catalytic activity seem to be attributable to other effects. Some conceivable reasons can be as follows:

(i) Different spatial distribution of Al atoms within the crystals of samples 18z and 20z. In case the outer crystal shell is enriched by Al one can expect a higher activity of such a sample compared with a sample containing uniformly distributed Al (active centers can be more easily accessible). However, this will be very difficult to prove as during the EDAX analysis the minimum diameter of the beam trace measured is much larger (about 1 μm) than that of the crystals.

(ii) The XRD phase analysis revealed that sample 20z contains a small amount of Y type zeolite (∼10%). The Si/Al ratio of Y zeolite is usually at least one order of magnitude smaller than that of MFI type material. Thus, the presence of Y zeolite in sample 20z could explain the lower number of Al atoms present in the MFI phase (i.e. the real Si/Al ratio of MFI is actually higher than that expected from the elemental analysis).

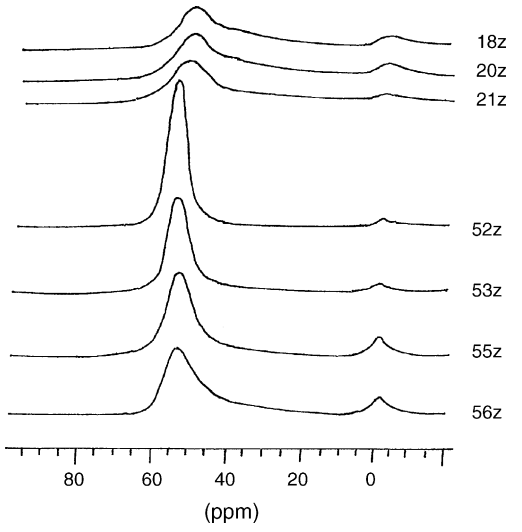

Fig. 3. ^{27}Al MAS NMR spectra of samples under study.

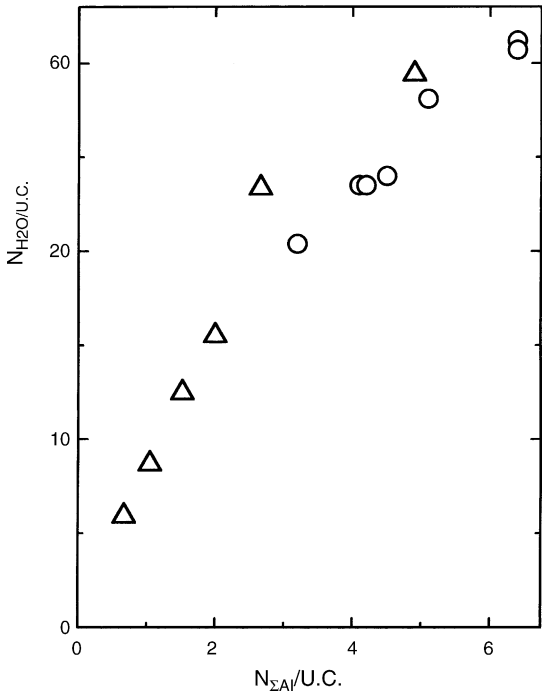

Fig. 4. Plot of the number of water molecules adsorbed per U.C. against total number of Al atoms per U.C.: (△)—literature data from Ref. [25], (○)—results of our measurements.

3.3. Immobilization of ethylene estimated from sorption and reaction dynamics

A deeper insight into immobilization of surface species in the zeolite channel system and their mobilization at elevated temperatures was obtained from the dependence of ethylene breakthrough curves and desorption curves of the products of its chemical transformation on the catalyst bed temperature. The breakthrough curves obtained from these experiments are shown in Fig. 6 for sample 20z.

At temperatures below 418 K no products of ethylene transformation were detected. Starting at 308 K a transient consumption of ethylene units occurred and increased with increasing temperature of the zeolite bed. At temperatures below 353 K a continuous breakthrough of ethylene was however still observed (for $t > 0$ the breakthrough curve did not reach the value $W_{et} = 0$). Between 353 K and 433 K the minimum on the breakthrough curves was for $t > 0$ at $W_{et} = 0$. Between 418 K and 453 K a temporary breakthrough of C_3–C_5 appeared in the form of a broad peak. A possible steady-state ethylene conversion and production of C_3–C_5 oligomers was below the detection limit. Starting from 473 K both the steady-state ethylene conversion and production of C_3–C_5 hydrocarbons was established.

The total amount of immobilized species was estimated from the mass balance of ethylene in the reactor. Each time we

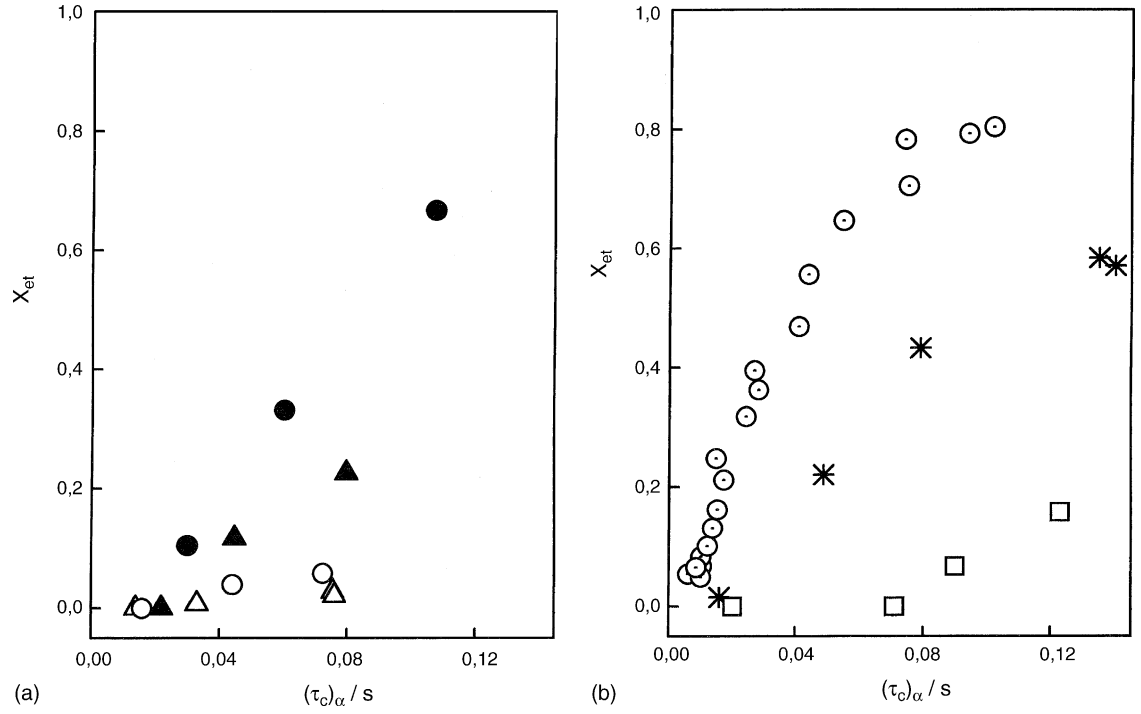

Fig. 5. Plots of ethylene conversion at 523 K against contact time for: (a) samples produced by VURUP: (△)—52, (▲)—53, (○)—55, (●)—56, (b) samples produced by CONTEKA: (⊙)—18z, (*)—20z, (□)—21z.

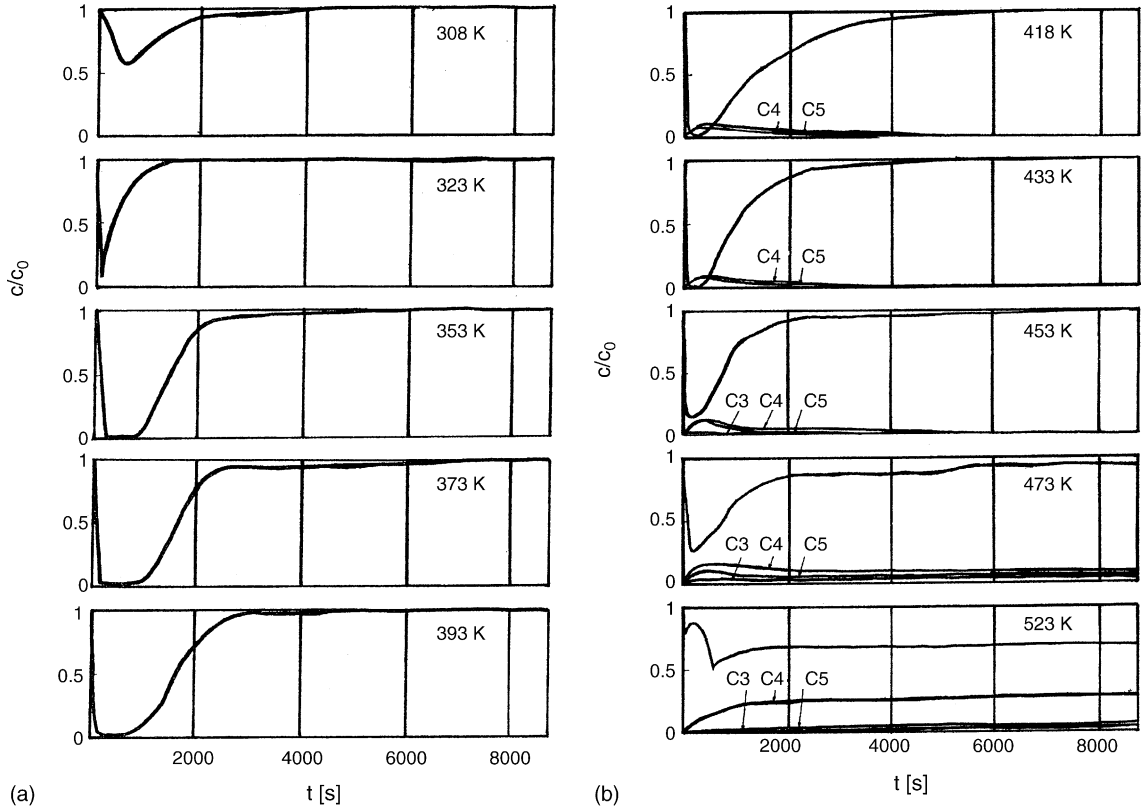

Fig. 6. The family of ethylene breakthrough curves obtained for sample 20z with catalyst bed temperature as a parameter: a—for temperature range 308–393 K, b—for temperature range 418–523 K: (●)—values obtained by GC analysis.

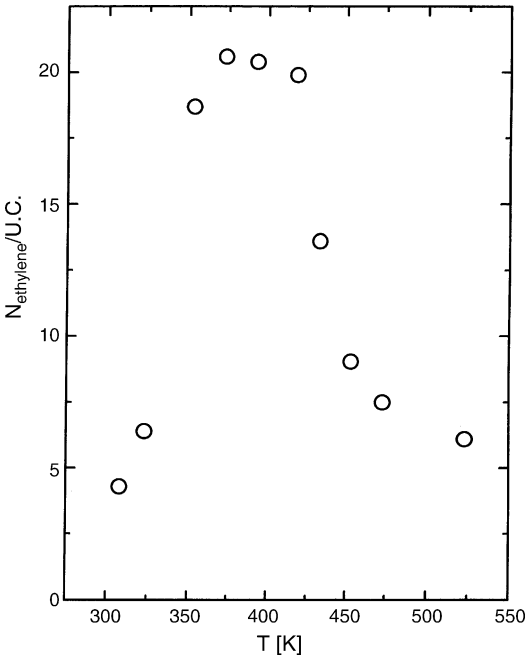

Fig. 7. Plot of the number of ethylene units ($N_{ethylene}$) trapped per unit cell of 20z sample, as a function of the catalyst bed temperature.

speak below of the trapped amount of immobilized species (or the number of immobilized molecules) we understand this quantity to be the amount of ethylene units (or the number of ethylene molecules). In the temperature region where no products of ethylene conversion were observed, the total amount of immobilized ethylene units was proportional to the area delimited by the axis of ordinates, the straight-line $c/c_o = 1$ and by the breakthrough curve W_{et} (t). Starting from 418 K the trapped amount of ethylene units was evaluated using Eq. (4) which accounts for the products of ethylene conversion. The number of ethylene units $N_{ethylene}$ trapped per U.C. plotted as a function of temperature is presented in Fig. 7. Below 353 K the amount of ethylene adsorbed in the bed increases steeply (and almost linearly) with increasing temperature. At 308 K the number of sorbed molecules is smaller than the number of aluminum atoms present in sample 20z.

The relatively slow consumption of ethylene in the aforementioned dynamic experiment (i.e. the relatively slow initial decrease of the ethylene breakthrough curve) and the fact that for $t > 0$ the minimum on the breakthrough curve lies at a relatively high ethylene concentration may be due to an autocatalytic step in oligomerization kinetics and/or to some effect of crystal channel blocking. The presence of the latter effect is indicated by a comparison of our dynamic sorption data with the results of static measurements of ethylene adsorption made by van den Berg [18] who found about 4.3 ethylene units per Al at room temperature. Owing to slow immobilization in the low-temperature region the dynamics of sorption loses the part of information normally contained in the tail of the dynamic curve; in other words, the process is so slow that it seemingly indicates attainment of the limiting concentration but in fact the pores are by far not filled by ethylene units. Thus, at bed temperature equal to 323 K the amount of trapped ethylene was found to correspond approximately to the number of Al atoms. A plausible explanation of the difference between the static and dynamic measurements would be that chain propagation proceeds rapidly at the lowest temperature and blocks the subsurface surface region of the crystals by a compact layer of oligomers.

Starting at 353 K a deviation from the linear increase takes place and a plateau is seen between 373 K and 418 K. This plateau corresponds to about 20 ethylene units/U.C. This shows a slightly lower degree of pore filling compared with that found for saturation of MFI zeolite with N_2 at 77 K (about 31 N_2 molecules/U.C.) [27]. Above 418 K a sharp decrease of $N_{ethylene}$ takes place, obviously due to cracking of hydrocarbon chains.

One should thus conclude that between 308 K and 418 K ethylene units are trapped due to a combined effect of ethylene adsorption and chain propagation. It appears that in the region of the plateau (373 K $< T <$ 418 K) some sort of saturation of the sample with trapped ethylene units was attained. We assume that in this temperature region two other processes accompany chain propagation: (i) increasing mobility of immobilized species may result in a release of adsorbed ethylene molecules, (ii) cracking reaction may set in and C_2H_4 originating in catalytic decomposition of oligomers may contribute to the total amount of ethylene detected. As no hydrocarbon higher than C_2 has been found in this temperature region, one can conclude that only β-cracking takes place and any bigger fragments after cracking remain immobilized in the channels of zeolite.

Another possibility is that in the aforementioned temperature region the channels are completely filled, there is still only a negligible rate of cracking and no hydrocarbon chain propagation takes place due to steric hindrances.

Above 418 K the resulting higher extent of cracking leads to a temporary occurrence of C_3, C_4 and C_5 hydrocarbons in the product.

Because of immobilization of long chain molecules in the channels of zeolite we have not found any molecules higher than C_5 in product. We have thus found mainly C_4 at the reactor outlet, expected to be the main product of C_6 cracking, and only lesser amounts of C_5 and C_3.

It should be also noted that in the temperature regions where the curves plotted as $N_{ethylene}$ versus the catalyst bed temperature exhibit the steepest positive and negative slope the ethylene breakthrough curves appear to be extremely unstable and exhibit damped oscillations as a response to even small system disturbances. The monotonous breakthrough curves presented in this study were obtained using specific precautions to maintain stable temperature and flow to avoid system disturbances.

Fig. 8 shows a plot of the apparent sorbed amount of water N_{H_2O} (N_{H_2O} is defined in Section 2.2) as a function of reaction temperature. Between 308 K and 393 K the plot in Fig. 8 is in some respects complementary to that presented in Fig. 7. However, at bed temperatures above 393 K the number of water molecules adsorbed is much higher than the number one would expect on the basis of the amount of adsorbed

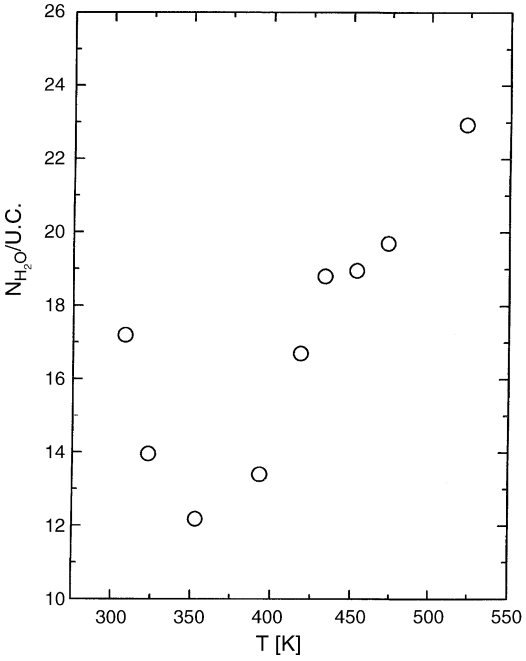

Fig. 8. Plot of the number of water molecules (N_{H_2O}) adsorbed per unit cell on the 20z zeolite preloaded with ethylene oligomerization intermediates.

hydrocarbon species. Assuming that at room temperature water does not displace the long-chain immobilized species, one can consider the amount of sorbed H_2O to be a measure of the intracrystalline void space that remains accessible to water molecules in the channel system. It appears that below 353 K the total amount of sorbed water and immobilized species, i.e. ~21 molecules per U.C., is considerably lower, than that found between 353 K and 433 K, i.e. 30–35 molecules per U.C. Above 433 K a small decrease in the total amount of adsorbed water and ethylene molecules has been observed, i.e. ~27 molecules per U.C. One can deduce that at temperatures of up to 353 K ethylene molecules immobilized in the outer crystal shell partially block the core of the crystals, which thus becomes inaccessible to water molecules. Above 353 K the increased mobility of the organic species in the reaction zone leads to a more compact filling of zeolitic channels by the oligomers formed. As a result the observed total number of sorbed species per U.C. passes through a maximum between 353 K and 418 K (cf. Fig. 7). The decrease in the total adsorbed amount of water and ethylene units observed above 433 K could be due to increased rate of cracking resulting in a decreased size of immobilized organic species in the crystals.

4. Conclusions

The curves plotted as ethylene conversion versus contact time were found to be sigmoid. This suggests that there is an autocatalytic step in the reaction scheme. At 623 K C_2–C_5 represent the main species present in the gas phase at the bed outlet. Only trace amounts of hydrocarbons higher than C_5 are present. Steady state occurrence of C_3–C_5 products takes place in the gas phase at temperatures higher than 453 K.

For catalysts exhibiting a comparable Si/Al ratio the reaction rate strongly depends on crystal size. It thus seems that the entire volume of the crystals (in particular of big ones) is not used for the catalytic transformation (the reaction is either diffusion limited or proceeds mainly on the outer crystal surface).

The shape of the ethylene breakthrough curves and the amount of ethylene immobilized in the catalyst estimated from dynamic measurements is strongly affected by the temperature of the bed. A characteristic local maximum on the ethylene breakthrough curve in its initial part appears to be due to an induction period of the oligomerization reaction. At 308 K the sorbed amount is lower than the aluminum content in HZSM-5 sample. With increasing reaction temperature the amount of immobilized species increases steeply, and a flat maximum corresponding to about 20 ethylene units per U.C. exists between 353 K and 418 K. A further increase of reaction temperature results in a rapidly decreasing amount of the immobilized species.

The amount of water adsorbed on samples preloaded with immobilized species plotted against the reaction temperature constitutes a curve to a certain extent complementary to the plot of immobilized species versus reaction temperature.

A relationship was established between the amount of immobilized ethylene units, the space accessible for water molecules on the catalyst with a partially mobilized layer of ethylene oligomers, and the temperature corresponding to the onset of continuous production of the catalytic bed. It appears that ethylene oligomerization catalyzed by HZSM-5 belongs to the class of reactions where the temperature onset of catalyst bed production is controlled by mobilization rate steps, which are represented in this particular case by cracking reactions.

Acknowledgements

This research was supported by Grant Agency of the Academy of Sciences of the Czech Republic via Project No IAA400400501. Support of this work within the framework of Czech–Polish interacademic exchange agreement is also acknowledged. The authors express their thanks to Mrs. J. Kudová for technical assistance and to Dr. J. Nováková from J. Heyrovský Institute of Physical Chemistry for measurements of TPD of NH_3.

References

[1] K. Beschmann, G.T. Kokotailo, L. Riekert, Chem. Eng. Process 22 (1987) 223.
[2] A. Zikánová, M. Derewinski, Zeolites 15 (1995) 148.
[3] A. Zikánová, J. Dubský, M. Derewinski, M. Kočiřík, Z. Phys. Chem. 189 (1995) 187.
[4] A. Micke, M. Bülow, M. Kočiřík, P. Struve, J. Phys. Chem. 98 (1994) 12337.
[5] M. Jama, M. Kočiřík, M. Eic, J. Dubský, A. Zikánová, M. Mello, A. Micke, in: M.M.J. Treacy, B.K. Marcus, M.E. Bisher, J.B. Higgins (Eds.), Proceedings of the 12th International Zeolite Conference, Baltimore, Maryland 1998, Materials Research Society Proceedings, Warrendale, PA, (1999), p. 215.

[6] M. Kočiřík, A. Zikánová, J. Dubský, P. Kroček, Coll. Czech. Chem. Commun. 59 (1994) 1001.
[7] M. Kočiřík, A. Micke, Langmuir 11 (1995) 3042.
[8] M. Derewiński, A. Zikánová, J. Kryściak, M. Kočiřík, Microporous Mesoporous Mater. 35–36 (2000) 367.
[9] L.M. Parker, D.M. Bibby, J.E. Patterson, Zeolites 4 (1984) 168.
[10] M. Soulard, S. Bilger, H. Kessler, J.L. Guth, Zeolites 7 (1987) 463.
[11] M. Soulard, S. Bilger, H. Kessler, J.L. Guth, Zeolites 11 (1991) 107.
[12] M. Soulard, S. Bilger, H. Kessler, J.L. Guth, Zeolites 11 (1991) 785.
[13] M. Soulard, S. Bilger, H. Kessler, J.L. Guth, Thermochim. Acta 167 (1992) 204.
[14] H. Ajot, C. Russmann, J.F. Joly, H. Kessler, Stud. Surf. Sci. Catal. 87 (1994) 477.
[15] J.L.P. van den Broeke, R. Krishna, Chem. Eng. Sci. 50 (1995) 2507.
[16] C.D. Chang, Hydrocarbons from Methanol, Marcel Dekker, New York, 1983.
[17] J. Nováková, L. Kubelková, Z. Dolejsek, P. Jiru, Coll. Czech. Chem. Commun. 44 (1979) 3341.
[18] J.P. van den Berg, J.P. Wolthuizen, A.D.H. Clague, G.R. Hays, R. Huis, G.R. van Hooff, J. Catal. 80 (1983) 130.
[19] J.P. van den Berg, J.P. Wolthuizen, G.R. van Hooff, J. Catal. 80 (1983) 139.
[20] V. Bolis, J.C. Vedrine, J.P. van den Berg, J.P. Wolthuizen, E.G. Derouane, J.C.S. Faraday I 76 (1980) 1606.
[21] E.G. Derouane, J.P. Gilson, J.B. Nagy, J. Mol. Catal. 10 (1981) 331.
[22] P. Dejaifve, J.C. Védrine, V. Bolis, E.G. Derouane, J. Catal. 63 (1980) 331.
[23] G. Spoto, S. Bordiga, G. Ricchiardi, D. Scarano, A. Zecchina, E. Borello, J.C.S. Faraday Trans. 90 (1994) 2827.
[24] R.Q. Snurr, A. Hagen, H. Ernst, H.B. Schwarz, J. Weitkamp, J. Kärger, J. Catal. 163 (1996) 130.
[25] S.N. Vereshchagin, N.P. Kirik, N.N. Shishkina, A.G. Anshits, Stud. Surf. Sci. Catal. 105 (1997) 1755.
[26] E. Alsdorf, M. Feist, H. Fichtner-Schmittler, Th. Gross, H.-J. Jerschkewitz, U. Lohse, B. Parlitz, Adsorpt. Sci. Technol. 5 (1988) 127.
[27] P.L. Llewellyn, J.-P. Coulomb, Y. Grillet, J. Patarin, G. Andre, J. Rouquerol, Langmuir 9 (1993) 1852.